

# The structures and dielectric properties of $\text{Ba}_{0.80}\text{Sr}_{0.20}\text{TiO}_3/\text{Pb}_{0.82}\text{La}_{0.18}\text{TiO}_3$ composite thick films with addition of $\text{PbO}-\text{B}_2\text{O}_3$ glass

Rong Wu, Piyi Du\*, Wenjian Weng, Gaorong Han

*State key lab of Silicon Materials, Zhejiang University, Hangzhou 310027, PR China*

Received 30 October 2004; received in revised form 2 March 2005; accepted 5 March 2005

Available online 16 April 2005

## Abstract

Sol-gel derived  $\text{Ba}_{0.80}\text{Sr}_{0.20}\text{TiO}_3$  (BST) and  $\text{Pb}_{0.82}\text{La}_{0.18}\text{TiO}_3$  (PLT) powders and a low-melting  $\text{PbO}-\text{B}_2\text{O}_3$  glass powder were mixed to prepare paste. The composite thick films ( $\sim 40 \mu\text{m}$ ) were fabricated by screen-printing the paste onto the  $\text{Al}_2\text{O}_3$  substrates with screen-printed silver bottom electrode and then sintered at the low temperature  $650-800^\circ\text{C}$ , respectively. X-ray diffraction (XRD), transmission microscope (TEM), scanning electron microscope (SEM) and an impedance analyzer were used to analyze the structures, microstructures and dielectric properties of the powders and the composite thick films. The results show that the composite thick films containing sol-gel derived  $\text{Ba}_{0.80}\text{Sr}_{0.20}\text{TiO}_3$  and  $\text{Pb}_{0.82}\text{La}_{0.18}\text{TiO}_3$  perovskite phases have been fabricated by using the  $\text{PbO}-\text{B}_2\text{O}_3$  glass as a sintering aid. Compared to conventional sintering at  $\geq 1200^\circ\text{C}$ , high densification of the composite thick films is achieved at temperature as low as  $800^\circ\text{C}$  by the “wetting” and “infiltration” of the liquid phase on the particles. The homogenization of the BST and PLT perovskite phase in the composite thick films is evitable by controlling the sintering temperature and time. The formation of the small amount of pyrochlore phase in composite thick films sintered at  $800^\circ\text{C}$  is resulted from both the volatilization of PbO and the interaction between the PLT and  $\text{PbO}-\text{B}_2\text{O}_3$  glass. The relative dielectric properties of the composite thick films exhibit good temperature-stable behavior, and the variation of the relative dielectric constant is less than 10% in the temperature range  $0-300^\circ\text{C}$ .

© 2005 Elsevier Ltd. All rights reserved.

**Keywords:** Perovskites; Composites; Films; Dielectric properties;  $\text{PbO}-\text{B}_2\text{O}_3$ ;  $(\text{Ba},\text{Sr})\text{TiO}_3$ ;  $(\text{Pb},\text{La})\text{TiO}_3$

## 1. Introduction

There is presently a growing commercial interest for miniaturized piezoelectric and pyroelectric transducers and actuators.<sup>1-4</sup> Thick films have recently been investigated as candidates for such applications because of the potential benefits of lower fabrication cost and better properties compared to thin film forms.<sup>5</sup> Lowering the sintering temperatures of the thick films is in demand in order to be compatible with the IC technology and to reduce manufacturing cost (energy consumption and Ag bottom electrode). The addition of a fluxing agent such as glass is an effective method that promotes

densification by liquid phase sintering<sup>6</sup> at low temperatures. Therefore, numerous kinds of glasses have been developed as sintering aids for ferroelectrics, such as  $\text{BaLiF}_3$ ,  $\text{PbO}-\text{B}_2\text{O}_3$ ,  $\text{PbO}-\text{Cu}_2\text{O}$ , etc.<sup>6-9</sup> The glass may act as a fluxing agent for liquid-phase sintering as well as a modifier of the dielectric properties. The extent of incorporation and the distribution of the incorporated atoms may alter the Curie temperature ( $T_c$ ), the sharpness of the transition, and the  $K$  value of the thick films. Therefore, glass compositions and chemical interaction between the glasses and the ceramic powders during the sintering process are very important factors in controlling the dielectric properties of the thick films.

Composites have shown great promise for the sensors and actuators because the electrical properties are predictable when the properties of the end members are known.<sup>10,11</sup> In

\* Corresponding author. Tel.: +86 571 87952324; fax: +86 571 87952341.  
E-mail address: [dupy@zju.edu.cn](mailto:dupy@zju.edu.cn) (P. Du).

addition, composites can overcome expositional limits since they have a wide composition range while other methods such as solid solutions are restricted by the ionic radius and valence state of the solute, which should be considered for a perfect solid solution and electrical neutrality.<sup>12,13</sup>

Attempts to synthesize a relaxor material conforming to X7R (EIA classifications) via compositional design have been unsuccessful. Attempts have also been made to synthesize heterogeneous relaxor materials where the different phases (such as PMN and BT) present give rise to different maxima in the permittivity-temperature response. Unfortunately, the high sintering temperature ( $\geq 1200^\circ\text{C}$ ) provides high  $\text{Pb}^{2+}$  ion mobility and homogenizes the various compositions, and the resultant dielectric response is a single peak corresponding to the dielectric characteristics of the average composition.<sup>14</sup>

$\text{Ba}_{1-x}\text{Sr}_x\text{TiO}_3$  and  $\text{Pb}_{1-x}\text{La}_x\text{TiO}_3$  are the most extensively investigated ferroelectrics to date because of their good dielectric and pyroelectric properties. Therefore, with a view to achieve high temperature stability of the dielectric and pyroelectric properties, composite thick films composed of  $\text{Ba}_{0.80}\text{Sr}_{0.20}\text{TiO}_3$  (BST) and  $\text{Pb}_{0.82}\text{La}_{0.18}\text{TiO}_3$  (PLT) have been manufactured by screen-printing the pastes onto the substrate, and in order to lower the sintering temperature and avoid the homogenization of the BST and PLT phase, the  $\text{PbO-B}_2\text{O}_3$  glass powder<sup>7</sup> was added into the paste. The dielectric properties and the factors affecting the dielectric anomaly are discussed from a microscopic viewpoint in this paper.

## 2. Experimental

PLT powder and BST powders with compositions of  $\text{Ba}_{0.80}\text{Sr}_{0.20}\text{TiO}_3$  and  $\text{Pb}_{0.82}\text{La}_{0.18}\text{TiO}_3$  were both synthesized using sol-gel process, respectively. The precursor materials used in preparation of PLT powder were the analytical grade  $\text{Pb}(\text{CH}_3\text{COO})_2 \cdot 3\text{H}_2\text{O}$ ,  $\text{La}(\text{NO}_3)_3$ , and  $\text{Ti}(\text{OC}_4\text{H}_9)_4$ . Lead acetate trihydrate was first dissolved in 2-methoxyethanol ( $\text{C}_3\text{H}_8\text{O}_2$ ) in a reaction flask at  $80^\circ\text{C}$  and then the solution was heated to  $118^\circ\text{C}$  for 4 h to remove the residual water. After cooling to  $80^\circ\text{C}$ , a stoichiometric amount of tetrabutyl titanate was added to the lead acetate solution and the solution was refluxed at  $124^\circ\text{C}$  for 3 h. After cooling the Pb-Ti complex alkoxide solution to room temperature, a stoichiometric amount of dehydrated lanthanum nitrate dissolved in  $\text{C}_3\text{H}_8\text{O}_2$  was added, and the Pb-La-Ti solution was stirred at room temperature. The concentration of the solution was adjusted to 0.2 M. The precursor materials used in the preparation of BST powder were the analytical grade  $\text{Ba}(\text{CH}_3\text{COO})_2$ ,  $\text{Sr}(\text{CH}_3\text{COO})_2$ , and  $\text{Ti}(\text{OC}_4\text{H}_9)_4$ . A stoichiometric amount barium acetate and strontium acetate were first dissolved in 2-methoxyethanol ( $\text{C}_3\text{H}_8\text{O}_2$ ) in a reaction flask at  $60^\circ\text{C}$  and then the solution was heated to  $118^\circ\text{C}$  for 1 h to remove the residual water. After cooling to  $60^\circ\text{C}$ , a stoichiometric amount of tetrabutyl titanate was added to

the Ba-Sr alkoxide solution and the Ba-Sr-Ti solution was stirred at room temperature. The concentration of the solution was adjusted to 0.1 M. Controlling the hydrolysis condition and adjusting the pH value of the solutions then obtained the Pb-La-Ti and Ba-Sr-Ti gels, which were freeze-dried to form the xerogels respectively. The Pb-La-Ti and Ba-Sr-Ti xerogels were calcined at  $850^\circ\text{C}$  for 2 h, respectively. The  $\text{PbO-B}_2\text{O}_3$  glass powder was synthesized by sintering the mixture of the analytical grade  $\text{PbO}$  and  $\text{HBO}_3$  at  $850^\circ\text{C}$  for 4 h, and down quenching the fluid into the de-ionized water followed. The  $\text{PbO}$  concentration of the  $\text{PbO-B}_2\text{O}_3$  glass is 65 mol%. The outcome was ball-milled for 24 h to obtain  $\text{PbO-B}_2\text{O}_3$  glass powder, and its melting point temperature is below  $650^\circ\text{C}$ .<sup>15</sup>

The as-synthesized PLT and BST powders were mixed to obtain the precursor powder according to the molar ratio of 1:1, and 8 wt%  $\text{PbO-B}_2\text{O}_3$  glass powder (relative to the precursor powder) was added into the precursor powder. A thick film paste was prepared by mixing the precursor powders (80 wt%) and an organic vehicle ( $\alpha$ -terpineol, butyl carbitol and ethyl cellulose) (20 wt%) on a ball mill using yttria-stabilized zirconia balls for 24 h to ensure thorough mixing of all of the constituent parts. The viscosity of the paste was controlled between 20 Pa s and 40 Pa s. Composite thick films were fabricated by screen-printing the paste on alumina ceramic substrates with silver bottom electrode, which was screen-printed on the alumina substrate and sintered at  $850^\circ\text{C}$  for 20 min. For all composite thick films,  $8^\circ\text{C}/\text{min}$  ramp-up and  $4^\circ\text{C}/\text{min}$  ramp-down rates were used after drying out the organic solvent in the composite thick films at  $250^\circ\text{C}$  for 6 h. The sintering temperatures of the screen-printing thick films were  $650^\circ\text{C}$ ,  $700^\circ\text{C}$ ,  $750^\circ\text{C}$  and  $800^\circ\text{C}$ , respectively, and the hold time was 30 min. To enable electrical measurements to be made through the composite thick films, silver top electrodes ( $\varnothing$  1 mm,  $0.79\text{ mm}^2$ ) were deposited onto the sintered composite thick films by using sputtering method.

The crystal structures of the PLT powder, BST powder,  $\text{PbO-B}_2\text{O}_3$  glass powder and the composite thick films were measured by using X-ray diffraction (XRD, Philips x'pert XRD system) with  $\text{Cu K}\alpha$  radiation. The microstructure of the PLT and BST powders were observed by using transmission microscope (TEM, JEOL CX-100). The microstructures of the composite thick films were observed by using scanning electron microscope (SEM, Hitachi SEM-S-570). The dielectric properties of thick films were analyzed by using an impedance analyzer (Agilent 4294A).

## 3. Results and discussion

### 3.1. Structural and microstructural characterization

Fig. 1 shows the single-phase perovskite structure for both BST and PLT powders after sintered at  $850^\circ\text{C}$  for 2 h and the amorphous structure for  $\text{PbO-B}_2\text{O}_3$  glass powder. All the

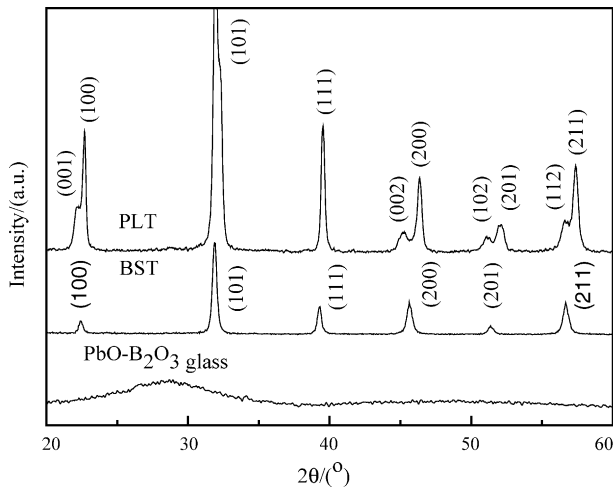


Fig. 1. XRD patterns for Ba<sub>0.80</sub>Sr<sub>0.20</sub>TiO<sub>3</sub> (BST) and Pb<sub>0.82</sub>La<sub>0.18</sub>TiO<sub>3</sub> (PLT) powders calcined at 850 °C and PbO–B<sub>2</sub>O<sub>3</sub> glass powder.

peaks can be identified according to JCPDS. The lattice parameters for the BST and PLT are very close. The structure of the PLT is typical tetragonal, and the lattice parameters are  $a = 3.9138 \text{ \AA}$  and  $c = 3.9980 \text{ \AA}$ , and the tetragonality is 1.02, which is smaller than that of the ceramics reported in literature ( $\sim 1.033$ ).<sup>16</sup> The reduction of the tetragonality is attributed to the grain size effect. For BST powder, the (1 0 0) and (0 0 1) peaks cannot be distinguished from each other, and neither the (2 0 0) and (0 0 2) peaks. The dielectric measurements show that the BST thick films have a  $T_c$  above room temperature. The structure of BST is therefore pseudocubic at the room temperature, and the lattice parameter is  $3.9774 \text{ \AA}$ . Fig. 2(a and b) gives the TEM micrographs and SADPs of the sol–gel synthesized BST and PLT powders sintered at 850 °C for 2 h. The particle sizes of the BST and PLT powders are both 200–400 nm.

Fig. 3 gives the XRD patterns for the composite thick films sintered at 650 °C, 700 °C, 750 °C and 800 °C for 30 min, respectively. The PLT retains its tetragonal phase in the composite thick films obviously. The lattice parameters of two phases remain very close in the composite thick films and

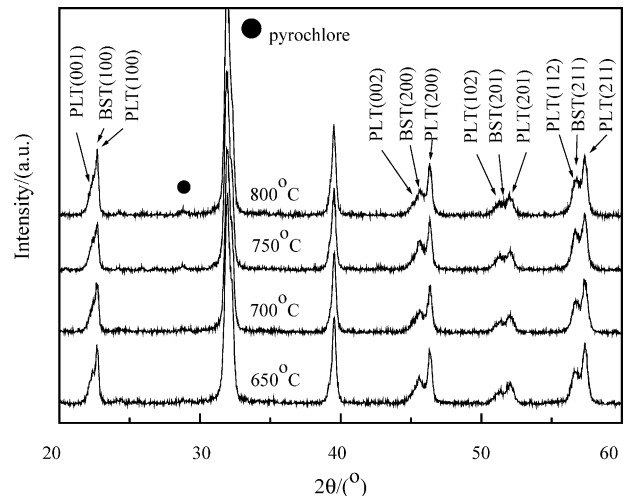


Fig. 3. XRD patterns for the composite thick films sintered at 650 °C, 700 °C, 750 °C and 800 °C for 30 min.

several peaks cannot be distinguished exactly, especially the peaks at  $2\theta = 22.6^\circ$  (PLT(1 0 0) and BST(1 0 0)),  $2\theta = 31.9^\circ$  (PLT(1 0 1) and BST(1 0 1)) and  $2\theta = 39.5^\circ$  (PLT(1 1 1) and BST(1 1 1)). Considering the composition of the thick films, each peak has been identified as shown in Fig. 3. No structural change is observed for the two phases in the composites thick films sintered at 650–700 °C. Pyrochlore phase appears in the composite thick films sintered above 750 °C, which is mainly attributed to both the volatilization of PbO and the diffusion between the PLT particles and the glass.<sup>9</sup>

Fig. 4(a–d) shows SEM micrographs of the surface morphologies of the composite thick films sintered for 30 min at different temperatures. It can be seen that there is a high level of porosity and the particles being loose in the composite thick films sintered at both 650 °C and 700 °C, although rather strong agglomerates were obtained in the composite thick films sintered at 700 °C. The microstructure of the composite thick films sintered at the 800 °C is illustrated in Fig. 4(c), which is represented by several features: residual pores, second phases and relatively good densified microstructure. The residual pores and the second phase are attributed to the low

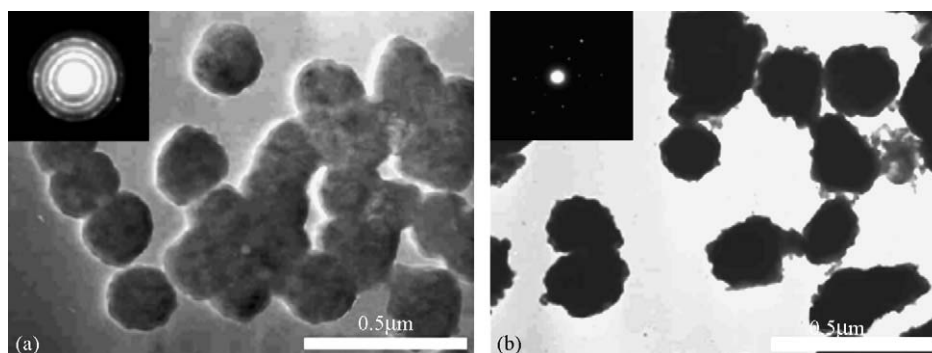


Fig. 2. TEM micrographs and SADPs of the sol–gel synthesized (a) BST and (b) PLT powders sintered at 850 °C for 2 h.

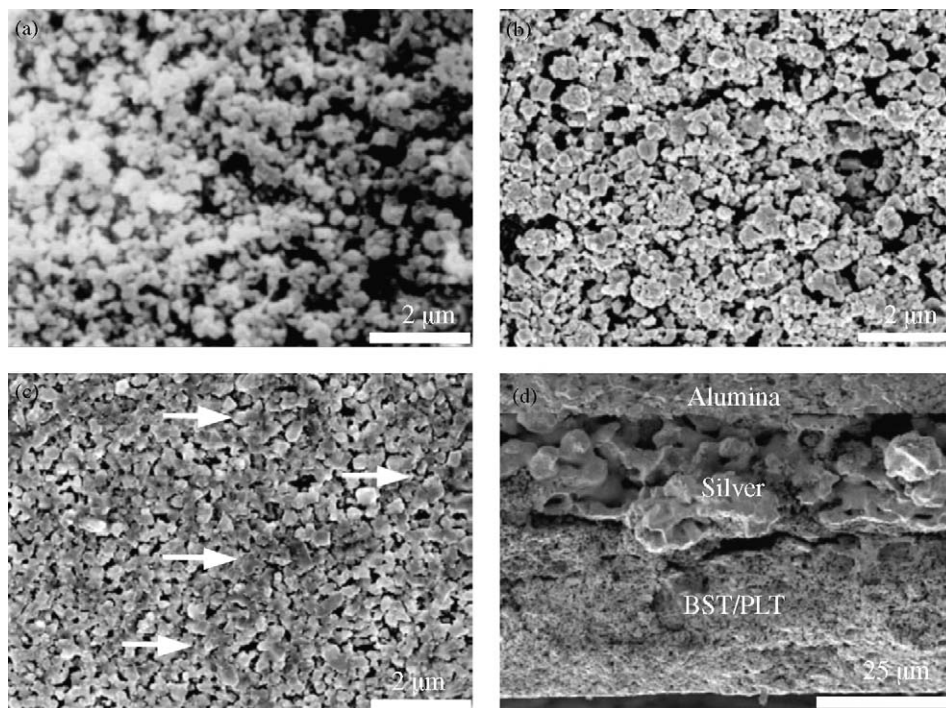


Fig. 4. SEM micrographs (SEI) of the surface morphologies of the composite thick films sintered at (a) 650 °C, (b) 700 °C and (c) 800 °C (the arrow pointed out the dark area) for 30 min, respectively, and (d) is the fracture surface of the composite thick films sintered at 800 °C.

green packing density of printed thick films and the formation of the liquid phase derived from the  $\text{PbO-B}_2\text{O}_3$  glass powder, respectively. Fig. 4(d) shows the SEM micrographs of the fracture surface of the composite thick film sintered at 800 °C. The composite thick films with uniform thickness of  $\sim 40 \mu\text{m}$  was obtained by the screen-printing and sintering.

### 3.2. Dielectric properties

Fig. 5(a and b) shows the relative dielectric constant ( $\epsilon_r$ ) and dielectric loss as a function of temperature of the composite thick films sintered at 650 °C, 700 °C, 750 °C and 800 °C, respectively, and the measurement frequency is 100 kHz. One can observe two maxima of the dielectric constant corresponding to two phase transitions ( $\sim 70^\circ\text{C}$  and  $\sim 169^\circ\text{C}$ ).

The Curie temperatures of the BST and PLT are both known to be dependent on the Sr and La content respectively, and the maxima at  $\sim 70^\circ\text{C}$  and  $\sim 169^\circ\text{C}$  are attributed to the phase transition of BST and PLT, respectively. The low-temperature maximum is very distinct for the composite thick films sintered at 650 °C, and disappear gradually with increasing the sintering temperature. The diffuseness of the dielectric peaks at  $\sim 169^\circ\text{C}$  increases with increasing the sintering temperature rapidly, which indicates a broadening phase transition occurring at  $\sim 169^\circ\text{C}$ . The temperature of the phase transition of the PLT phase is agree with the conclusions of Iijima et al.<sup>17</sup> that the difference of 1 mol% of La concentration in PLT compositions changes the phase transition temperature in 18 °C. The existence of the residual pores and the low  $\epsilon$  second phase lower the relative dielectric constant of the

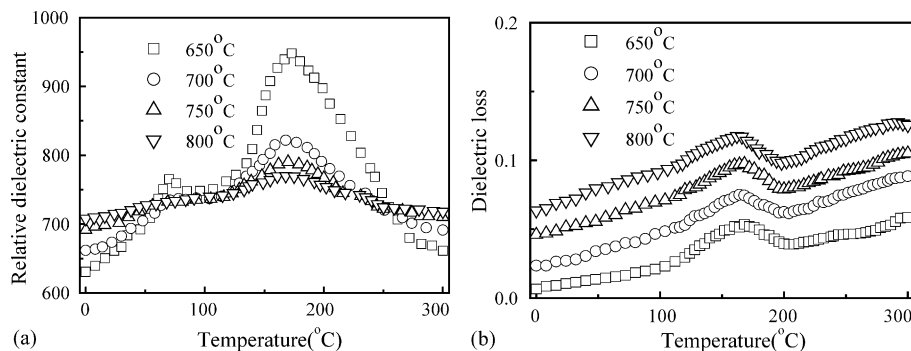


Fig. 5. (a) Relative dielectric constant and (b) dielectric loss as a function of temperature for the composite thick films sintered at different temperatures. The measurement frequency is 100 kHz.

composite thick films compared with the thick films without glass addition. The dielectric loss is higher than that of the BST thick films<sup>18</sup> and increase as increasing the sintering temperature. This can be explained by the defects generated by the interaction between the BST/PLT and the glass.

The  $\varepsilon$  versus temperature  $T$  relation shows a deviation from the Curie–Weiss Law. Smolenskii<sup>19</sup> introduced the concept of a Gaussian distribution of the Curie temperatures characteristic to the small microregions considered noncorrelated. Using this approach, the calculated dielectric constant is approximated by a Gaussian Law,

$$\varepsilon = \varepsilon_m \exp \left[ -\frac{(T - T_m)^2}{2\delta_1^2} \right] \quad (1)$$

where  $\varepsilon$  is the dielectric constant,  $\varepsilon_m$  is its maximum value,  $T_m$  the temperature corresponding to this maximum, and  $\delta_1$  the Gaussian coefficient of diffuseness. Although this law was used to describe the diffuse phase transition (DPT) for many relaxor, it has the limit to characterize only a complete DPT. In order to describe the dielectric properties of systems not showing complete DPT, another approximate empirical equation was proposed by Uchino and Nomura.<sup>20</sup>

$$\frac{1}{\varepsilon} = \frac{1}{\varepsilon_{\max}} + \frac{(T - T_{\max})^\gamma}{2\varepsilon_{\max}\delta_2^\gamma} \quad (2)$$

where  $\gamma=1$  corresponds to the conventional Curie–Weiss law, and  $\gamma=2$  to a completely DPT, while  $1 < \gamma < 2$  is reported for systems with intermediate degrees of diffuseness. The parameter  $\delta_2$  has the dimension of a temperature only when  $\gamma=2$ , indicating in this case the temperature extension of the phase transition. The diffuseness of a phase transition can be described by a parameter  $\gamma$ , called the diffuseness exponent, which can be obtained by fitting the high-temperature dielectric data (for  $T > T_{\max}$ , where  $T_{\max}$  is the temperature corresponding to the peak in the  $\varepsilon$ – $T$  spectrum) to the Eq. (2). The dielectric peaks at  $\sim 169^\circ\text{C}$  in Fig. 5a is analogous to that of the bulk PLT. From Eq. (2) the diffuseness exponent  $\gamma$  of the dielectric peak at  $\sim 169^\circ\text{C}$  is obtained and shown in Table 1. The temperature stability of the relative dielectric constant in the temperature range 0–300 °C improved obviously, which is mainly attributed to the diffuseness of the dielectric peak at  $\sim 169^\circ\text{C}$ . The variation of the relative dielectric constant of the composite thick films sintered at different temperature were shown in Table 1, and that of the

composite thick films sintered at 800 °C is less than 10% in the temperature range 0–300 °C.

### 3.3. Influence of the PbO–B<sub>2</sub>O<sub>3</sub> glass

A further discussion point is derived from the fact that the use of the flux agent will affect the thick films' dielectric properties due to the existence of low dielectric constant phase and the interactions between the BST/PLT and the PbO–B<sub>2</sub>O<sub>3</sub> glass.

The interactions between BST/PLT and the PbO–B<sub>2</sub>O<sub>3</sub> glass play a very important role on the microstructures and dielectric properties of the composite thick films. The reduction of the tetragonality of the PLT phase caused by the diffusion between the PLT phase and the liquid phase have been reported in other authors' paper.<sup>9</sup> The defects in PLT phase resulted in the formation of the pyrochlore phase. Pb–O–Pb networks are connected to B<sub>2</sub>O<sub>3</sub> networks via BO<sub>4</sub> tetrahedra in the PbO-containing glasses, and the structure of the glass is much looser than that of the crystal phase. The Pb<sup>2+</sup> ions in PLT phase can diffuse into the liquid phase when the sintering temperature is relatively high. However, when a very thin diffusion layer of composition inhomogeneity is formed, it is difficult to measure a concentration gradient in these diffusion layers. To avoid the homogenizing the composition of the composite thick films, the sintering temperatures are  $\leq 800^\circ\text{C}$ , and the calcinations time is 30 min.

The temperatures used to sinter the composite thick films are  $\leq 800^\circ\text{C}$ , which is too low to start the solid-state sintering process ( $\geq 1200^\circ\text{C}$ ). The densification of the composite thick films is attributed to the liquid-phase sintering by using the PbO–B<sub>2</sub>O<sub>3</sub> glass aids. Comparison of Fig. 4(a–c) emphasizes that the viscosity of the liquid phase reduces largely at the higher sintering temperature. After the densification process, liquid-sintering process aids remain at the grain boundaries as a second phase (the dark area in Fig. 4(c)). Therefore, the level of the porosity gradually decreased as increasing the sintering temperature. While the “infiltration” and “wetting” of the liquid phase on the particles are dominant in the composite thick films sintered at 800 °C, the sintering kinetics is liquid-phase sintering rather than solid-state sintering. Physically, this translates into a large difference in the exhibited grain size. Particularly attention was paid to the variation of the particle sizes of the thick films sintered at different temperature. The particle sizes of the BST and PLT powders are both 200–400 nm, respectively, which were obtained from the TEM micrographs showed in Fig. 2(a and b). The strong agglomerates of the particles disturb the estimate of the grain size in the thick films, and the appearance of large particles might be the agglomerate of the small ones. The variation of grain size affected by the liquid phase will be reported in future.

The dielectric properties of the composite thick films represent those of the components BST and PLT in the composite thick films. However, the interaction between the BST/PLT and the glass during sintering process modified the dielectric

Table 1

The diffuseness exponent  $\gamma$ ,  $T_{\max}$ ,  $\varepsilon_{\max}$  of the dielectric peak at  $\sim 169^\circ\text{C}$  and  $\Delta\varepsilon/\varepsilon$  (0–300 °C) corresponding to the composite thick films sintered at different temperature

Sintering temperature (°C)	$\varepsilon_{\max}$	$T_{\max}$	$\gamma$	$\Delta\varepsilon/\varepsilon$ (%)
650	945	170	1.3	47
700	822	168	1.4	24
750	790	169	1.6	14
800	770	168	1.8	9

properties of the composite thick films. It is observed that the phase transitions ( $\sim 169^\circ\text{C}$ ) of the composite thick films sintered at all temperatures are broadened, and the diffuseness of the dielectric peak increases as increasing the sintering temperature. The densification of the composite thick films was improved with increasing the sintering temperature, which give rise to the slight increase of the relative dielectric constants of the composite thick films. However the interdiffusion between the BST/PLT and the glass reduce the maximum values of the relative dielectric constants largely. Therefore, the maximum values of the relative dielectric constants decrease but the relative dielectric constants at  $0\text{--}50^\circ\text{C}$  increases as increasing the sintering temperatures.

When PT is modified by  $\text{La}^{3+}$  ions, cation vacancies are created to keep the charge neutrality, producing a mixture of two distinct vacant sites (Pb-site and/or Ti-site vacancies), and the nature of these cation-site vacancies had pronounced effects on the characteristics of ferroelectricity and that the microcompositional inhomogeneity caused by the Ti-site vacancy is primarily responsible for the manifestation of the relaxor behavior from normal ferroelectricity in PLT.<sup>21</sup> Moreover, the depolarization field and short-range force will decrease the ordering of the dipoles in the small ferroelectric particles and as a result the phase transition of the PLT is also affected by the small particle size.<sup>22</sup> In view of these, it can be concluded that the potential fluctuations and the structural defects generated by diffusion have mainly effects on the phase transition of the PLT phase.

The flattening of the dielectric peaks at  $70^\circ\text{C}$  is ascribed to the interaction between the BST and the glass. Firstly, Previous work<sup>23,24</sup> have showed that the internal stress due to the grain size effect plays a very important role to diffuse the transition for fine grained (less than  $1\ \mu\text{m}$ ) barium titanate. The grain size of BST in composite thick films is less than  $400\ \text{nm}$ , and the internal stress due to the grain size effect is very significant. Besides, the probability of compositional fluctuation in a system containing two phases of ferroelectric solid solution is very large. The compositional fluctuation in BST microregions may be enhanced by the defects generated by the interaction between BST and the glass.

In summary, the interactions between the PLT/BST and the  $\text{PbO-B}_2\text{O}_3$  glass are the major factors affecting the broadening the phase transition of the PLT and BST and hence high temperature stability of the relative dielectric constant was achieved.

#### 4. Conclusion

Composite thick films containing sol-gel derived  $\text{Ba}_{0.80}\text{Sr}_{0.20}\text{TiO}_3$  and  $\text{Pb}_{0.82}\text{La}_{0.12}\text{TiO}_3$  perovskite phases have been fabricated by using the  $\text{PbO-B}_2\text{O}_3$  glass sintering aid. Compared to conventional sintering at  $\geq 1200^\circ\text{C}$ , high densification of the composite thick films is achieved at temperature as low as  $800^\circ\text{C}$  by the “wetting” and “infiltration”

of the liquid phase on the particles. The homogenization of the BST and PLT perovskite phase in the composite thick films is evitable by control the sintering temperature and time. The formation of the small amount of pyrochlore phase in composite thick films sintered at  $800^\circ\text{C}$  is resulted from both the volatilization of  $\text{PbO}$  and the interaction between the PLT and  $\text{PbO-B}_2\text{O}_3$  glass. The relative dielectric properties of the composite thick films exhibit good temperature-stable behavior, and the variation of the relative dielectric constant is less than 10% in the temperature range  $0\text{--}300^\circ\text{C}$ .

Further work is required to investigate the pyroelectric properties of the composite thick films sintered with addition of  $\text{PbO-B}_2\text{O}_3$  glass for use in pyroelectric detectors in a wide temperature range.

#### Acknowledgements

This work is supported by the Natural Science Foundation of China under contract nos. 50372057 and 50332030, and by Chinese National Key Project for Fundamental Researches under grant no. 2002CB613302, respectively.

#### References

1. Park, S. E. and Shrout, T. R., Ultrahigh strain and piezoelectric behavior in relaxor based ferroelectric single crystals. *J. Appl. Phys.*, 1997, **28**, 1804–1811.
2. Moreno-Gobbi, A., Perez, M., Negreira, C. A., Garcia, D. and Eiras, J. A., Ultrasonic attenuation and elastic modulus of ferroelectric ceramics. *Scripta. Mater.*, 2000, **43**, 259–263.
3. Lucat, C., Menil, F. and Von Der Mühl, R., Thick film densification for pyroelectric sensors. *Meas. Sci. Technol.*, 1997, **8**, 38–41.
4. Wu, R., Du, P. Y., Weng, W. J. and Han, G. R., Low temperature preparation of the temperature-stable BST/PLT composite thick films. *Chin. J. Inorg. Mater.*, 2004, **19**, 1099–1104.
5. Corker, D. L., Zhang, Q., Whatmore, R. W. and Perrin, C., PZT ‘composite’ ferroelectric thick films. *J. Eur. Ceram. Soc.*, 2002, **22**, 383–390.
6. Corker, D. L., Whatmore, R. W., Ringgaard, E. and Wolny, W. W., Liquid-phase sintering of PZT ceramics. *J. Eur. Ceram. Soc.*, 2000, **20**, 2039–2045.
7. Sarkar, S. K. and Sharma, M. L., Liquid phase sintering of  $\text{BaTiO}_3$  by boric oxide ( $\text{B}_2\text{O}_3$ ) and lead borate ( $\text{PbB}_2\text{O}_4$ ) glasses and its effect on dielectric strength and dielectric constant. *Mater. Res. Bull.*, 1989, **24**, 773–779.
8. Wang, S. F., Yang, T. C., Huebner, W. and Chu, J. P., Liquid phase sintering and chemical inhomogeneity in the  $\text{BaTiO}_3\text{--BaCO}_3\text{--LiF}$  system. *J. Mater. Res.*, 2000, **15**, 407–416.
9. Singh, S., Thakur, O. P. and Chandra, P., Influence of liquid phase additives on structural and sintering behaviour of samarium modified lead titanate ceramics. *J. Electroceram.*, 2003, **11**, 67–72.
10. Hollingsworth, M. D., Crystal engineering: from structure to function. *Science*, 2002, **295**, 2410–2413.
11. Wu, Y. J., Uekawa, N. F., Sasaki, Y. and Kakegawa, K., Microstructures and pyroelectric properties of multicomposition  $0.9\text{PbZrO}_3\cdot x\text{PbTiO}_3\cdot(0.1-x)\text{Pb}(\text{Zn}_{1/3}\text{Nb}_{2/3})\text{O}_3$  ceramics. *J. Am. Ceram. Soc.*, 2002, **85**, 1988–1992.
12. Sohn, J. H., Cho, J. W., Lee, J. H. and Cho, S. H., Strong ferroelectric perovskite phase in Pb-containing composites. *Solid State Ionics*, 1998, **108**, 141–149.

13. Kobayashi, T., Shimanuki, S., Saito, S. and Yamashita, Y., Improved growth of large lead zinc niobate titanate piezoelectric single crystals for medical ultrasonic transducers. *Jpn. J. Appl. Phys.*, 1997, **36**, 6035–6038.
14. Tavernor, A. W., Li, H. P. and Stevens, R., Production and characterisation of composite relaxor ferroelectric multi-layer structures. *J. Eur. Ceram. Soc.*, 1999, **19**, 1859–1863.
15. Levin, E. M. and McMurdie, H. F., *Phase diagrams for ceramists 1975 supplement compiled at the National Bureau of Standards*. The American Ceramic Society, Ohio, 1964, p. 122.
16. Keizer, K. and Burggraf, A. J., Grain size effects on the ferroelectric–paraelectric transition, the dielectric constant, and the lattice parameters in lanthana-substituted lead titanate. *Phys. Status Solidi A*, 1974, **26**, 561–569.
17. Iijima, K., Takayama, R., Tomita, Y. and Ueda, I., Epitaxial growth and the crystallographic, dielectric, and pyroelectric properties of lanthanum-modified lead titanate thin films. *J. Appl. Phys.*, 1986, **60**, 2914–2919.
18. Su, B., Holmes, J. E., Meggs, C. and Button, T. W., Dielectric and microwave properties of barium strontium titanate (BST) thick films on alumina substrates. *J. Eur. Ceram. Soc.*, 2003, **23**, 2699–2703.
19. Smolenskii, G. A., Physical phenomena in ferroelectrics with diffused phase transition. *J. Phys. Soc. Jpn.*, 1970, **28**, 26–37.
20. Uchino, K. and Nomura, S., Critical exponents of the dielectric constants in diffused phase transition crystals. *Ferroelectrics*, 1982, **44**, 55–61.
21. Kim, T. Y. and Jang, H. M., B-site vacancy as the origin of spontaneous normal-to-relaxor ferroelectric transitions in La-modified PbTiO<sub>3</sub>. *Appl. Phys. Lett.*, 2000, **77**, 3824–3826.
22. Zhoua, Q. F., Chan, H. L. W., Zhang, Q. Q. and Choy, C. L., Raman spectra and structural phase transition in nanocrystalline lead lanthanum titanate. *J. Appl. Phys.*, 2001, **89**, 8121–8126.
23. Arlt, G., Hennings, D. and de With, G., Dielectric properties of fine-grained barium titanate ceramics. *J. Appl. Phys.*, 1985, **58**, 1619–1625.
24. Fang, T. T., Hsieh, H. Y. and Shiau, F. S., Effects of pore morphology and grain size on the dielectric properties and tetragonal-cubic phase transition of high-purity barium titanate. *J. Am. Ceram. Soc.*, 1993, **76**, 1205–1211.